

Automatic quantitative characterization of rapid protein dynamics in live cell microscopy assays

James SJ Lee¹, Samuel V. Alworth¹, Chi-Chou Huang¹, Seho Oh¹, Hirotada Watanabe², Kazuki Horikawa³, Takeharu Nagai³

¹DRVision Technologies LLC, 15921 NE 8th St. Suite 200, Bellevue, WA 98008, USA

²Nikon Instruments Company, Yokohama-city, Kanagawa Japan

³Research Institute for Electronic Science, Hokkaido University, Sapporo Japan

Introduction

Biological reactions depend largely on the diffusion and localization of biomolecules and intracellular organelles. A new generation of microscope and fluorescent probe technologies has enabled the visualization of rapid protein dynamics and molecular and subcellular events. However, quantitative characterization of biomolecule and intracellular organelle mobility is challenging since the dynamics of objects are complex and may be obscured over time. Therefore, much of the kinetic characterization is based on manual tracking and interpretation, which is tedious, subjective and irreproducible.

We have developed automatic subcellular object tracking and characterization technologies including 1) a highly robust and flexible tracking method called "soft tracking"; 2) track refinement and state detection; and 3) kinetic characterization. We include new kinetic measurements such as track zones of influence, counts of fast/slow objects, counts of "Association" and "Disassociation" states. The objective of this study is to validate the performance of the technologies using live cell images of photo-convertible, fluorescent protein Phamret (Photoactivation-Mediated Resonance Energy Transfer) fused to SKL tripeptide for peroxisome localization.

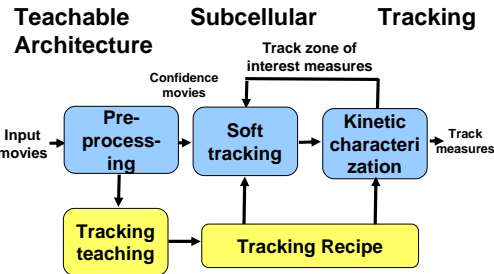


Fig 1. Teachable subcellular tracking architecture consists of a preprocessing step, a soft tracking step and a kinetic characterization step. It is implemented in SVCell™ kinetic prototype.

Input movie(s) are pre-processed to generate confidence maps. The high confidence map regions are then detected. The morphology, kinetic and object states are considered to produce track candidates and to match objects into track segments.

The soft tracking and kinetic characterization can be taught by a tracking teaching step to generate tracking recipe that can be applied to multiple input movies for kinetic high content screening.

Pre-processing

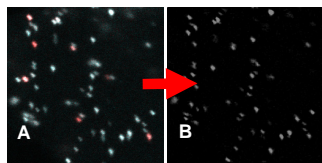


Fig 2. Pre-processing is performed by adaptive processing¹ to generate a high confidence map using teachable structure guided processing². (A) shows a representative image frame from the study movie. (B) shows the confidence map.

State Based Soft Tracking

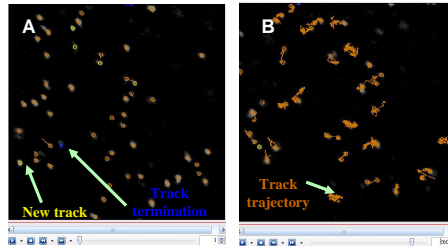


Fig 3. Soft tracking method (A) detect new tracks and detect track termination, (B) track objects over time

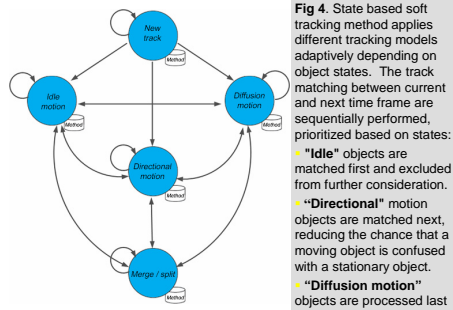


Fig 4. State based soft tracking method applies different tracking models adaptively depending on object states. The track matching between current and next time frame are sequentially performed, prioritized based on states: • "Idle" objects are matched first and excluded from further consideration. • "Directional" motion objects are matched next, reducing the chance that a moving object is confused with a stationary object. • "Diffusion motion" objects are processed last

$$\begin{aligned} \vec{V}_p &= (x_i[t-1] - x_i[t-2], y_i[t-1] - y_i[t-2]) \\ \vec{V}_i &= (x_i[t] - x_i[t-1], y_i[t] - y_i[t-1]) \\ \text{and } \vec{V}_{av} & \text{ is the average of } \vec{V}[t-1] \text{ for all track in } [t-1] \text{ frame} \end{aligned}$$

The matching scoring model is different with the tracking states

Idle: $TScore_{id} = \text{Flash}(\vec{V}; \vec{0}, \vec{0}, \vec{R}_{idle})$

Directional: $TScore_{di} = \text{Flash}(\vec{V}; \vec{V}_p, \vec{V}_i, \vec{R}_{direction})$

Diffusion: $TScore_{df} = \text{Flash}(\vec{V}; \vec{0}, \vec{0}, \vec{R}_{diffusion})$

Default: $TScore_{df} = \max\{\text{Flash}(\vec{V}; \vec{V}_p, \vec{V}_i, \vec{R}_{direction}), \text{Flash}(\vec{V}; \vec{0}, \vec{0}, \vec{R}_{diffusion})\}$

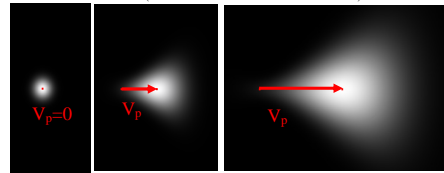


Fig 5. The matching score model Flash(a,b,c,d) is a flash light like distribution which is a function of velocity

Track Zone of Influence Measures

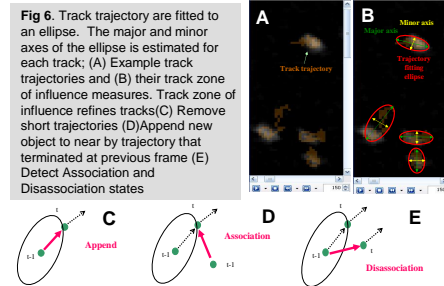


Fig 6. Track trajectory are fitted to an ellipse. The major and minor axes of the ellipse is estimated for each track; (A) Example track trajectories and (B) their track zone of influence measures. Track zone of influence refines tracks (C) Remove short trajectories (D) Append new object to near by trajectory that terminated at previous frame (E) Detect Association and Disassociation states

Soft Tracking Teaching

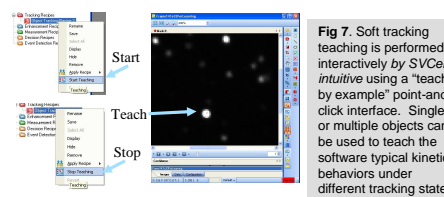


Fig 7. Soft tracking teaching is performed interactively by SVCell™ intuitive using a "teach by example" point-and-click interface. Single or multiple objects can be used to teach the software typical kinetic behaviors under different tracking states

Study Materials and Methods

Our hypothesis is that our methods achieve similar performance to the best manual method. The manual tracks are created independently by two analysts and discrepancies are resolved through review with the group. We test the hypothesis using tracking accuracy metrics.

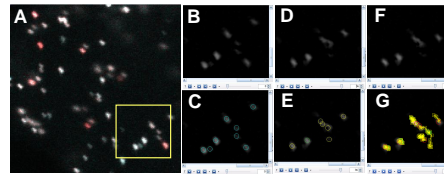


Fig 8. (A) Test movie containing live cell images of photo-convertible, fluorescent protein Phamret (Photoactivation-Mediated Resonance Energy Transfer) fused to SKL tripeptide for peroxisome localization. 48 objects are tracked over a 298 frame movie. (B) Shows the confidence map of the region highlighted in yellow frame at time frame "0". (C) Circle overlays show the tracked objects at time frame "0". (D) Shows the confidence map of the region highlighted in yellow frame at time frame "36". (E) Circle overlays show the tracked objects at time frame "36". (F) Shows the confidence map of the region highlighted in yellow frame at time frame "39". (G) Show the tracks from time frame "0" up to time frame "39".



Tracking Accuracy Metrics

Average track error: No. of tracks having $\geq 10\%$ incorrect tracking time points over the entire time divided by the total number of tracks

Average object tracking error: No. of incorrect tracking time points over the entire time divided by the total number of time points

Average matching tracking sensitivity: For each truth trajectories, no. of objects in the detected tracks having $\geq 10\%$ overlay with the truth trajectories divided by all objects in the truth trajectories

Results

We used manual tracks as the truth and evaluated the tracking performance using the tracking accuracy metrics. Since the manual tracks are subject to human drawing errors and the automatic detection also introduce additional errors, we used "radial limit" from 1 to 5 pixels in both x and y locations for applying tracking accuracy metrics. We believe the results at "radial limit" of 5 pixels can appropriately reflect the tracking performance.

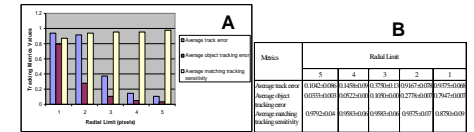


Fig 9. (A) The plots of tracking accuracy metrics for different radial limits. (B) Table of the numerical values of the metrics. Note that at radial limit of 5 pixels, the Average track error is 0.10420±0.086, the Average object tracking error is 0.0333±0.003 and the Average matching tracking sensitivity is 0.9792±0.04

Conclusion

Study results show that the tracking results are closely aligned with the manual tracks. We conclude that our tracking technologies support the hypothesis with statistical significance as the 95% confidence levels have little error and high sensitivity. We believe the technologies have broad applications, and are working to validate them on a number of live cell assays.

Literature cited

- Alworth SV, Oh S, Cheng Y, Lee JSJ. 2007. Learnable analysis module for subcellular, time lapse microscopy assays. Poster presented at the 2007 Society for Neuroscience conference in San Diego, CA.
- Lee JSJ. 2002. Structure-guided image processing and image feature enhancement. United States patent number 6,463,175 .

Future Efforts

- We will continue to test these methods using different types of experimental images from additional assays
- We will further incorporate motion energy to improve the tracking

Acknowledgments

This research was supported in part by grant no. 1R43GM07774-01 from the NIGMS